Journal of Materials Chemistry C

Accepted Manuscript

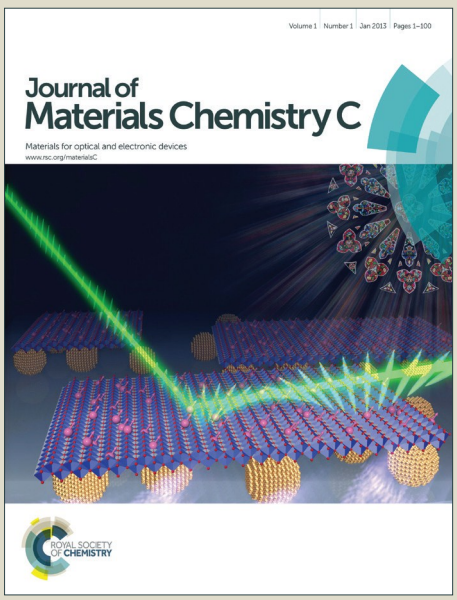

ROYAL SOCIETY OF CHEMISTRY

www.rsc.org/materialsC

Substituent Position Engineering of Diphenylquinoline-based Ir(III) Complexes for Efficient Orange and White PhOLEDs with High Color Stability/Low Efficiency Roll-Off Using Solution-Processed Emission Layer

Ganguri Sarada,[‡a] Juho Yoon,[‡a] Woosum Cho,[a] Minji Cho,[b] Daw Won Cho,[b] Sang Ook Kang,[b] Yeonsig Nam,[c] Jin Yong Lee,[c] and Sung-Ho Jin*[a]

[a] Department of Chemistry Education, Graduate Department of Chemical Materials, BK 21 PLUS Team for Advanced Chemical Materials, and Institute for Plastic Information and Energy Materials, Pusan National University, Busan, 609-735, Republic of Korea,

[b] Department of Advanced Materials Chemistry, Korea University, Sejong-city 339-700, Republic of Korea

[c] Department of Chemistry, Sungkyunkwan University, Suwon 440-746, Republic of Korea

[‡] These authors contributed equally to this work

*Corresponding Author E-mail: shjin@pusan.ac.kr

Abstract: Three new heteroleptic Ir(III) complexes ***o*-LIrpic**, ***m*-LIrpic**, and ***p*-LIrpic** (L=CF_3DPQ) consisting of 2,4-diphenylquinoline (DPQ) with a -CF_3 group at ortho (*o*)/ meta (*m*)/ para (*p*) positions of the metalated phenyl ring, respectively, as the main ligands were synthesized and used as emitters in phosphorescent organic light-emitting diodes (PhOLEDs). We realized that -CF_3 position extremely affects the crucial photophysical and electronic properties such as emission color, photoluminescence quantum yield (PLQY) and energy levels of these Ir(III) complexes resulting in -CF_3 position-dependent performance of their PhOLEDs. To verify the effect of -CF_3 group position on device performance, three other Ir(III) complexes ***o*-LIrtmd**, ***m*-LIrtmd**, and ***p*-LIrtmd** were synthesized using the same main ligands but different ancillary ligand. In the two series of Ir(III) complexes, the devices with *m*-CF_3 based complexes are outstanding in performance compared to *o*- or *p*-CF_3 based ones due to the enhanced PLQY and well suppressed non-radiative deactivations by *m*- substitution. Finally, the single emission layer solution-processed orange and two-component white PhOLEDs fabricated using ***m*-LIrpic** as orange emitter achieved the maximum external quantum efficiency of 17.1% (43.9 cdA^{-1}) and 21.1% (48.8 cdA^{-1}), respectively, with highly stable color coordinates and low efficiency roll-off. This is the highest efficiency reported to date for solution-processed orange PhOLEDs using small molecular host with easily accessible emitter.

1. Introduction

Highly efficient orange phosphorescent heavy-metal complexes are indispensable for the fabrication of monochromatic displays and two-component or full color white organic light-emitting diodes (WOLEDs).[1] Among the heavy-metal complexes, iridium(III) complexes are considered as the most promising phosphors in OLEDs mainly due to their high spin-orbit coupling (SOC) and the ease of functionalization of cyclometalating (C^N) ligands to control the emission colors.[2] In recent years, orange phosphorescent OLEDs (PhOLEDs) using Ir(III) complex emitters have achieved high external quantum efficiency (EQE) of about 28% in vapor deposition process.[3] Conversely, the solution-process is most preferred method due to its low processing cost and large scale application for practical utility.[4] But the availability of highly soluble orange Ir(III) complex emitters with easy synthetic routes are scarce and also the efficiencies of their solution-processed PhOLEDs are laid far behind those of the vacuum-deposited ones to date.[5] Until now, the highest EQE reported for solution-processed orange PhOLEDs with Ir(III) complex [Ir(Flpy-CF_3)$_3$] emitter was 17.6% with Commission Internationale de L'Eclairage (CIE) coordinates (0.531, 0.466).[5b] However, here a dendrimeric host was used which restricts the usage of higher generation dendrimers due to their voltage dependent-poor carrier mobilities. Also the synthesis of the C^N ligand was achieved by multi-steps which limits its application in large scale.[6]

2,4-Diphenylquinoline (DPQ)-based C^N ligands are exhibited as promising candidates for developing efficient orange/orange-red Ir(III) complexes for solution-processed PhOLEDs due to their elevated electron-affinities, ease of synthesis and high solubility without the need of any

alkyl chains.[7] Based on this, recently we demonstrated a series of solution-processable Ir(III) complexes with different C^N ligands containing of phenylquinoline moiety.[7a] Amongst, the orange PhOLEDs with emitter $(DPQ)_2Ir$(pic-N-O) showed maximum EQE of 14.2% in a ternary host system compared to the other (perfluorinatedphenyl-, fluorenyl-, and carbazoyl-phenylquinoline ligand based) Ir(III) complexes owing to its relatively high photoluminescence quantum yield (PLQY), which illustrates the advantage of DPQ ligand over the other C^N ligands in designing efficient phosphors. On the other hand, the energy levels of the emissive states (^{3}MLCT and/or ^{3}LC) of the Ir(III) complexes can be effectively modified to obtain wide-ranging emission colors and PLQYs by the substituent effects such as electron withdrawing or electron donating on C^N ligands and also by the substituent position effects.[2c,7h] As far as we know, fine-tuning of PLQY and photophysical/electronic properties and hence the PhOLED performance of the Ir(III) complexes by a simple control of the substituent position on C^N ligand has not been much investigated.

With the aim to develop novel orange Ir(III) complexes that are easy to access synthetically, possesses high PLQY and good solubility for realization of highly efficient solution-processed PhOLEDs in practical applications, we selected DPQ as C^N ligand driven by its flexible color tunabilitiy. In this paper, we introduced trifluoromethyl ($-CF_3$) group at ortho (*o*)/ meta (*m*)/ para (*p*) positions (Fig. 1) of the metalated phenyl ring of DPQ and synthesized Ir(III) complexes with two different ancillary ligands in order to validate the effect of $-CF_3$ position on the electronic structure of the Ir(III) complexes and consequently on performance of PhOLEDs. We realized that the location of $-CF_3$ is very important in attaining high device performance. In particular, the orange PhOLED fabricated with solution-processed emission layer using the *m*-CF_3 linked Ir(III) complex, ***m*-LIrpic**, as dopant achieved the maximum EQE of 17.1% with CIE coordinates

(0.528, 0.469), this is the highest EQE among the solution-processed orange PhOLEDs using small molecular host system (see Table S1, summary of the reported device performances) and also this result is similar to the highest efficiency reported using dendrimeric host.[5b] Furthermore, the two-component white PhOLEDs fabricated with ***m*-LIrpic** as orange component demonstrated maximum EQE of 21.1%. The detailed approach and the results are discussed hereafter.

2. Results and discussion

2.1 Synthesis and Characterization

The -CF_3 functionalized C^N ligands ***o*-L**, ***m*-L**, and ***p*-L** (L=CF_3DPQ) based on DPQ skeleton were prepared in single step by the acid-catalyzed Friedlander condensation reaction[7d] of two commercially available starting materials. The new Ir(III) complexes ***o*-LIrpic**, ***m*-LIrpic**, ***p*-LIrpic** and ***o*-LIrtmd**, ***m*-LIrtmd**, ***p*-LIrtmd** were prepared readily following the syntheses of the intermediate dichloro-bridged dimers and the reaction of the corresponding dimer with ancillary ligands picolinate (pic) or 2,2,6,6-tetramethylheptane-3,5,-diketonate (tmd) in presence of Na_2CO_3 base (Scheme S1). All the Ir(III) complexes have been characterized by ^1H, ^{13}C NMR, and high resolution mass spectroscopy [Fig. S1-S2 in Supporting Information (SI)]. The new Ir(III) complexes have good solubility in common organic solvents such as chloroform ($CHCl_3$), tetrahydrofuran, and chlorobenzene (CB).

2.2 Thermal and Photophysical Properties

Thermal properties of the Ir(III) complexes were evaluated using thermogravimetric analysis (TGA) under N_2 atmosphere with a scanning rate of $10^oC\ min^{-1}$. The TGA curves (Fig. S3a in SI) of all the Ir(III) complexes exhibited reasonable thermal stabilities with decomposition temperatures (T_d), corresponding to 5% weight loss, over 300-370^{o}C.

In order to examine the effect of -CF_3 group position on ground and excited state properties of the Ir(III) complexes, UV–visible absorption (Fig. 2a & 2b) and the photoluminescence (PL) spectra (Fig. 2c & 2d) were measured in $CHCl_3$ (10^{-5} M) at room temperature. The stronger absorption peaks between 265 and 350 nm mostly represent the ligand centered $^1\pi$-π^* transitions. The weaker absorption peaks between 350 and 520 nm are known to be the admixed ^{1}MLCT and ^{3}MLCT/ ^{3}LC transitions where the usually spin-forbidden transitions of the triplet states are allowed due to the strong SOC induced by the iridium metal.[8] As shown in Fig. 2a and 2b, the lower energy transition bands of ***m*-LIrpic** and ***m*-LIrtmd** are clearly blue shifted compared to the *o*- and *p*- analogs indicating the impact of -CF_3 substitution position on the ground state properties of the Ir(III) complexes.

Insets in Fig. 2c and 2d represent emission colors of the Ir(III) complexes after UV-irradiation in $CHCl_3$. All the Ir(III) complexes emit an intense orange/orange-red/red color upon photo-excitation. The structureless emission pattern of these Ir(III) complexes indicates ^{3}MLCT character of the emissive excited state.[9] The position of -CF_3 on DPQ has marked changes in the emission wavelengths of both the series of Ir(III) complexes. The PL peaks are recorded at 602, 565, 574 nm and 623, 593, 598 nm for ***o*-LIrpic**, ***m*-LIrpic**, ***p*-LIrpic** and ***o*-LIrtmd**, ***m*-LIrtmd**, ***p*-LIrtmd**, respectively. Similar to the lower energy bands in absorption spectra, the PL_{max} of ***m*-LIrpic** is hypsochromic shifted around 37 nm and 9 nm compare to the ***o*-LIrpic** and ***p*-LIrpic**, respectively. The -CF_3 group at *m*- location lowers the highest occupied molecular orbital (HOMO) level of ***m*-LIrpic** leading to blue shift in emission.[10,11] The strong polarization effect and the large steric volume of the -CF_3 substituent at *o*- position might be further reasons for variation in the electronic distribution of ***o*-LIrpic** when compared to ***p*-LIrpic**.[12] Similar

tendencies in PL were also observed for ***o*-LIrtmd**, ***m*-LIrtmd**, and ***p*-LIrtmd** demonstrating the influence of -CF_3 group position on emission color tuning.

As shown in Fig. S3b, the trends in film state emission spectra of all the Ir(III) complexes were comparable to those of measured in $CHCl_3$ except that the former are red shifted about 12-25 nm in case of ***o*-LIrpic**, ***m*-LIrpic**, ***p*-LIrpic** and 4-7 nm in ***o*-LIrtmd**, ***m*-LIrtmd**, ***p*-LIrtmd**. The well-known reason for less red shift in tmd based Ir(III) complexes is the bulky *t*Bu groups which suppress the intermolecular interactions responsible for bathochromic shift in solid state emission.[13] The PLQYs of ***o*-LIrpic**, ***m*-LIrpic**, ***p*-LIrpic** and ***o*-LIrtmd**, ***m*-LIrtmd**, ***p*-LIrtmd** are 0.27, 0.65, 0.57 and 0.18, 0.41, 0.37, respectively, measured in dichloromethane (CH_2Cl_2) at room temperature using rhodamine B ($\Phi_f = 0.68$) as a standard. The transient PL analyses were carried out for estimating the emission lifetimes of the Ir(III) complexes in CH_2Cl_2 at room temperature and in 2-methyltetrahydrofuran (2-MeTHF) at 77 K (Fig. S4 and Table 1). The decay profiles of all the Ir(III) complexes are monoexponential with short emission lifetimes ranging from 2.0-2.5 μs for ***o*-LIrpic**, ***m*-LIrpic**, ***p*-LIrpic** and 1.6-2.0 μs for ***o*-LIrtmd**, ***m*-LIrtmd**, ***p*-LIrtmd** in CH_2Cl_2 representing the phosphorescence as origin of the emission.[14] In order to gain insight into the root cause for variation in PLQYs of the Ir(III) complexes, the relaxation dynamics such as radiative and non-radiative decay rate constants (K_r/K_{nr}) were calculated from the obtained lifetimes. In accordance with the energy gap law,[15] the *m*-CF_3 based Ir(III) complexes exhibited relatively lower K_{nr} and higher PLQYs compared to the *o*- or *p*-CF_3 based Ir(III) complexes for both the series demonstrating the substituent position effect on the emissive properties of the Ir(III) complexes.

2.3 Electrochemical & Theoretical Calculations

Cyclic voltammetry (CV) measurements were carried out to study the -CF_3 group position effect on the redox properties and subsequently on the frontier orbitals of the six Ir(III) complexes. As depicted in Fig. S5, the oxidation potentials of *m*-CF_3 complexes are positive-shifted in comparison with *o*- and *p*-CF_3 analogs. As a result, the HOMO levels of *m*- based Ir(III) complexes are noticeably stabilized (see Table 1) causing the enhancement in band gaps. The CV characteristics of all the Ir(III) complexes are in good agreement with the photophysical properties. Hence, it is worth noting that a change in the location of -CF_3 does affect the redox properties of these Ir(III) complexes. In order to gain insight into the structure–property relationships, density functional theory (DFT) calculations for all the Ir(III) complexes were carried out and the optimized HOMOs and LUMOs of these Ir(III) complexes were shown in Fig. S6. Throughout the six Ir(III) complexes, the delocalization of HOMOs were mostly distributed over the Ir(III) metal center and the metalated phenyl ring of DPQ, whereas the LUMOs are mostly located on quinoline and partly on both the phenyl rings of the C^N ligands.

2.4 Electroluminescent properties of PhOLEDs

With the aim to elucidate the -CF_3 group position effect on EL properties of the new Ir(III) complexes, monochromatic PhOLEDs were fabricated using the following optimized device configuration: ITO/PEDOT:PSS (40 nm)/TAPC:DCzPPy:emitter (10 wt%, 40 nm)/TmPyPB (50 nm)/LiF (1 nm)/Al (100 nm), where TAPC is 1,1-bis(4-methylphenyl)-aminophenyl-cyclohexane, DCzPPy is 2,6-*bis*(3-(carbazol-9-yl)phenyl)pyridine, and TmPyPB is 1,3,5-tris(*m*-pyrid-3-ylphenyl)benzene. In all the devices, TAPC:DCzPPy acts a mixed host, PEDOT:PSS serves as hole injection layer (HIL), TmPyPB as electron transport layer (ETL), indium-tin oxide (ITO) as anode and LiF/Al as the electron injection layer and cathode. Device structure and the energy levels of the materials involved in the fabrication of monochromatic PhOLEDs

are given in Fig. 3a. Confinement of the excitons in emitting layer (EML) is expected since the triplet energy (T_1)[16] of TAPC (T_1=2.87 eV) and DCzPPy (T_1=2.71 eV) are higher than all the Ir(III) complexes (T_1 ~ 2.08-2.21 eV, see Fig. S7a). TAPC is a unipolar (hole transporting) and DCzPPy a bipolar (more electron transporting, less hole transporting) materials. Therefore, the molar ratio of TAPC:DCzPPy was optimized to 4:6, respectively, for better charge balance. EML was spin coated using CB solvent and ETL, LiF and Al were vacuum deposited on top of it. The PL spectra of neat TAPC, DCzPPy, and TAPC:DCzPPy films are given in Fig. S7b. As demonstrated in Fig. 3b and 3c, the deep overlap of the emission spectrum of TAPC:DCzPPy with the MLCT absorption region of all Ir(III) complexes ensures an efficient energy transfer from the mixed host to the Ir(III) complexes.[17]

The surface morphology for thin films of the mixed host (TAPC:DCzPPy) and TAPC:DCzPPy doped with 10 wt% Ir(III) complex were analyzed using atomic force microscopy (AFM). As shown in Fig. S8, the root-mean-square (RMS) surface roughness of the doped EML films were similar to the undoped TAPC:DCzPPy films and even better in case of ***m*-LIrpic** and ***m*-LIrtmd** doped films. The current density-voltage- luminance (J-V-L) and EQE-luminance (η-L) of the PhOLEDs based on ***o*-LIrpic**, ***m*-LIrpic**, and ***p*-LIrpic** dopants are represented in Fig. 4a and 4b. The maximum luminance of the devices are 1592 cdm^{-2} for ***o*-LIrpic**, 4062 cdm^{-2} for ***m*-LIrpic**, and 3710 cdm^{-2} for ***p*-LIrpic**. The highest EQE of 17.1% (43.9 cdA^{-1}, 23.0 lmW^{-1}) was demonstrated by the PhOLED with ***m*-LIrpic**, while the ***p*-LIrpic** and ***o*-LIrpic** showed 12.8% (30.1 cdA^{-1}, 13.5 lmW^{-1}) and 8.9% (13.2 cdA^{-1}, 5.2 lmW^{-1}), respectively. Furthermore, a low efficiency roll-off was recorded for ***m*-LIrpic** based device with an EQE of about 14.7% at 1000 cdm^{-2}, i.e efficiency is retained up to 86%. The results of the monochromatic PhOLEDs are summarized in Table 2. The device architecture also has an

important role in the high performance of ***m*-LIrpic** along with its good photophysical properties. It could be explained by considering the HOMO levels of these Ir(III) complexes where a moderate barrier of 0.15 eV exists for hole transfer from the TAPC to the ***m*-LIrpic**, while the remaining complexes do not have any such barrier. It is well known that the electron mobility in organic materials is generally several orders of magnitude lower than the hole mobility.[18] From this, we strongly believe that the moderate hole barrier of ***m*-LIrpic** [0.15 eV] balances the injection of holes in line with electrons, therefore, a high recombination of hole-electron is anticipated. In addition, introduction of $-CF_3$ at *m*- position highly suppressed the non-radiative deactivations and improved the PLQY of the *m*-CF_3 based complexes which resulted high efficiency in PhOLEDs.

In order to validate the aforementioned effect of $-CF_3$ group position on device performance, PhOLEDs with another series of emitters ***o*-LIrtmd**, ***m*-LIrtmd**, and ***p*-LIrtmd** contains tmd ancillary ligand were fabricated using the similar device configuration. Fig. 5a and 5b represent the J-V-L and η-L plots of the PhOLEDs with these Ir(III) complexes. Though the device structure and the main ligands are same, the performance of ***o*-LIrpic**, ***m*-LIrpic**, and ***p*-LIrpic** based devices are outstanding compared to the ***o*-LIrtmd**, ***m*-LIrtmd**, and ***p*-LIrtmd** based devices. It is beyond the scope of this paper to examine the exact reasons for the low performance of 'tmd' based PhOLEDs, however, it could be partly due to the low PLQY of these Ir(III) complexes. Interestingly, the trends in efficiency of ***o*-LIrtmd**, ***m*-LIrtmd**, and ***p*-LIrtmd** based devices follow the structure–property relationships similar to the ***o*-LIrpic**, ***m*-LIrpic**, and ***p*-LIrpic**. Accordingly, the PhOLEDs with ***m*-LIrtmd** show superior EQE of 6.4% (11.3 cdA^{-1}, 5.5 lmW^{-1}) than ***p*-LIrtmd** with 5.0% (7.5 cdA^{-1}, 3.4 lmW^{-1}) and ***o*-LIrtmd** with 3.7% (3.0 cdA^{-}

^{1}, 1.2 lmW^{-1}). In this scenario, it is worth stating that a subtle change in the substituent ($-CF_3$) position on DPQ has profound impact on the PhOLED device performance.

EL spectra of the six PhOLEDs at 30 $mAcm^{-2}$ are shown in Fig. S9. Though the bandwidths are broadened in EL spectra, but the EL_{max} are comparable to their PL_{max}. These variations in the spectral bandwidth of EL compared with PL are expected to be caused by the difference in the excitation process of the Ir(III) complexes.[19] The absence of any residual emission from TAPC:DCzPPy in EL spectra of the devices imply an effective energy transfer from the mixed host to the Ir(III) complexes. The CIE coordinates of the monochromatic PhOLEDs are represented in Fig. 6 and those are (0.624, 0.375), (0.535, 0.461), (0.566, 0.432) for ***o*-LIrpic**, ***m*-LIrpic**, ***p*-LIrpic** and (0.664, 0.334), (0.596, 0.403), (0.622, 0.377) for ***o*-LIrtmd**, ***m*-LIrtmd**, ***p*-LIrtmd**, respectively at 30 $mAcm^{-2}$. The confinement of the recombination zone to the EML and the charge balance in the mixed host system are well indicated by the stable CIE coordinates of the PhOLEDs where the shift is just (0.001, 0.001) with increasing luminance as shown in Fig. S10.[20] From the above data, it is interesting that the PhOLEDs with ***m*-LIrpic** and ***p*-LIrpic** show orange color, ***m*-LIrtmd** shows orange-red, ***o*-LIrpic** and ***p*-LIrtmd** show red color, and ***o*-LIrtmd** shows deep-red color.

From the high performance of ***m*-LIrpic** based orange and **[$(dfpmpy)_2Ir(EO_2$-pic)]** based blue PhOLEDs,[21] it is likely to attain high efficiency in solution-processed white OLEDs using these materials as two-component emitters. Therefore, we fabricated white PhOLEDs with single EML using ternary host system consisting of poly(vinylcarbazole) (PVK)/N,N-dicarbazolyl-3,5-benzene (mCP)/2,2′-(1,3-phenylene)bis[5-(4-tert-butylphenyl)-1,3,4-oxadiazole (OXD-7) with the configuration (see Fig. S11): ITO/PEDOT:PSS-4083 (40 nm)/PVK:mCP:OXD-7 (37.5:37.5:25) (85 wt%):blue:orange (x:y) (15 wt%) (50 nm)/1,3,5-tri(1-phenyl-1H-

benzo[d]imidazol-2-yl)phenyl (TPBi) (30 nm)/LiF (1 nm)/Al (100 nm), where the doping ratios of blue:orange were systematically optimized to 17:0.01 (device **W1**) and 17:0.015 (device **W2**). **W1** demonstrated a maximum EQE of 21.1% at 2000 cdm^{-2} with a peak luminance of 12992 cdm^{-2}, also, it exhibited low roll-off in efficiency with EQE 17.3% at 3000 cdm^{-2} (Fig. 7). Very importantly, the color coordinates of **W1** are highly stable with $\Delta CIE_{x,y}$ (0.007, 0.009), which is nearly independent of the driving voltage as shown in Fig. 8. All the data of white PhOLEDs are summarized in Table 3, Fig. 7 and S12. Exchange of the HIL from PEDOT:PSS-4083 to the low conductivity PEDOT:PSS-8000 might have a great potential for further enhancement of device performance due to the improved charge balance.[5b,22] In conclusion, to the best of our knowledge, high EQE with very low roll-off up to 3000 cdm^{-2} simultaneously ultra-high color stability in a single EML white PhOLEDs fabricated by solution-process are seldom reported.[23,5b] Finally, it is worth stating that both the orange and white PhOLEDs fabricated with the orange phosphor ***m*-LIrpic** exhibited an excellent device performance in two separate host systems credited to the good phophysical properties and solution processability of the new orange emitter.

3. Conclusion

In this work, we introduced $-CF_3$ group at three different positions (*o-* /*m-* /*p-*) on 2,4-diphenylquinoline (DPQ) cyclometalating ligand and synthesized two series of highly soluble new heteroleptic Ir(III) complexes ***o*-LIrpic**, ***m*-LIrpic**, ***p*-LIrpic** and ***o*-LIrtmd**, ***m*-LIrtmd**, ***p*-LIrtmd** for usage in solution-processed PhOLEDs. We observed that introduction of $-CF_3$ into *m-* position highly diminished the non-radiative relaxations and improved the PLQY of the *m*-CF_3 based Ir(III) complexes and also tuned the emission color from red to orange. As a result, the performance of monochromatic PhOLEDs with both the series of Ir(III) complexes follows

the order: *m* > *p* > *o*. Particularly, the orange PhOLED fabricated with solution-processed emission layer using ***m*-LIrpic** as dopant in a simple mixed host achieved the maximum efficiency of 17.1% with low efficiency roll-off and almost constant CIE coordinates (0.528, 0.469). Furthermore, the two-component white PhOLEDs using ***m*-LIrpic** as orange emitter showed a peak EQE of 21.1% with strikingly low efficiency roll-off with 17.3% at 3000 cdm^{-2} and highly stable color with ΔCIEx,y (0.007, 0.009). The overall results of these orange and white PhOLEDs are among the best ones in solution-processed devices. These findings demonstrate a simple approach in fine-tuning the emissive properties of the Ir(III) complexes in order to obtain highly efficient PhOLEDs for practical application of solution-process.

Acknowledgments

This work was supported by grant fund from the National Research Foundation (NRF) (2011-0028320) and the Pioneer Research Center Program through the NRF (2013M3C1A3065522) by the Ministry of Science, ICT & Future Planning (MSIP) of Korea.

References

1 [a] S. Reineke, M. Thomschke, B. Lüssem and K. Leo, *Rev. Mod. Phys*., 2013, **85**, 1245; [b] C. Fan, L. Zhu, B. Jiang, Y. Li, F. Zhao, D. Ma, J. Qin and C. Yang, *J. Phys. Chem.* C, 2013, **117**, 19134; [c] C.-C. Chen, H.-Y. Lin, C.-H. Li, J.-H. Wu, Z.-Y. Tu, L.-L. Lee, M.-S. Jeng, C.-C. Lin, J.-H. Jou and H.-C. Kuo, *International Journal of Photoenergy*, *Volume 2014*, Article ID 851371, 6 pages.

2 [a] Y. H. Lee, J. Park, S.-J. Jo, M. Kim, J. Lee, S. U. Lee and M. H. Lee, *Chem. Eur. J*., 2015, **21**, 2052; [b] D. Liu, H. Ren, L. Deng and T. Zhang, *ACS Appl. Mater. Interfaces,*

2013, **5**, 4937; [c] Q.-L. Xu, X. Liang, S. Zhang, Y.-M. Jing, X. Liu, G.-Z. Lu, Y.-X. Zheng and J.-L. Zuo, *J. Mater. Chem. C,* 2015, **3**, 3694.

3 [a] G. Li, Y. Feng, T. Peng, K. Ye, Y. Liu and Y. Wang, *J. Mater. Chem. C*, 2015, **3**, 1452; [b] G. Li, D. Zhu, T. Peng, Y. Liu, Y. Wang and M. R. Bryce, *Adv. Funct. Mater*., 2014, **24**, 7420; [c] R. Wang, D. Liu, H. Ren, T. Zhang, H. Yin, G. Liu and J .Li, *Adv. Mater.*, 2011, **23**, 2823; [d] H.-H. Chou, Y.-K. Li, Y.-H. Chen, C.-C. Chang, C.-Y. Liao and C.-H. Cheng, *ACS Appl. Mater. Interfaces*, 2013, **5**, 6168.

4 [a] X. Liu, S. Wang, B. Yao, B. Zhang, C.-L. Ho, W.-Y. Wong, Y. Cheng and Z. Xie, *Org. Electron*., 2015, **21**, 1; [b] R. Wang, D. Liu, R. Zhang, L. Deng and J. Li, *J. Mater. Chem*., 2012, **22**, 1411; [c] T. Giridhar, T.-H. Han, W. Cho, C. Saravanan, T.-W. Lee and S.-H. Jin, *Chem. Eur. J*., 2014, **20**, 8260.

5 [a] K. S. Yook and J. Y. Lee, *Adv. Mater*., 2014, **26**, 4218; [b] B. Zhang, G. Tan, C.-S. Lam, B. Yao, C.-L. Ho, L. Liu, Z. Xie, W.-Y. Wong, J. Ding and L. Wang, *Adv. Mater*., 2012, **24**, 1873; [c] C. Fan and C. Yang, *Chem. Soc. Rev.*, 2014, **43**, 6439; [d] H. Xu, R. Chen, Q. Sun, W. Lai, Q. Su, W. Huang and X. Liu, *Chem. Soc. Rev.*, 2014, **43**, 3259; [e] C.-L. Ho, W.-Y. Wong, G.-J. Zhou, B. Yao, Z. Xie and L.Wang, *Adv. Funct. Mater.*, 2007, **17**, 2925; [f] C. Fan, J. Miao, B. Jiang, C. Yang, H. Wu, J. Qin and Y. Cao, *Org. Electron.*, 2013, **14**, 3392.

6 [a] D. A. Markelov, Y. Y. Gotlib, A. A. Darinskii, A. V. Lyulin and S. V. Lyulin, *Polym. Sci.*, Ser. *A*, 2009, **51**, 331; [b] J. M. Lupton, I. D. W. Samuel, R. Beavington, M. J. Frampton, P. L. Burn and H. Bässler, *Phys. Rev. B*, 2001, **63**, 155206.

7 [a] J. Park, J.-S. Park, Y. G. Park, J. Y. Lee, J. W. Kang, J. Liu, L. Dai and S.-H. Jin, *Org. Electron.*, **2**013, **14**, 2114; [b] J. Ding, J. Lü, Y. Cheng, Z. Xie, L. Wang, X. Jing and F. Wang, *Adv. Funct. Mater*., 2008, **18**, 2754; [c] Z. Ma, J. Ding, B. Zhang, C. Mei, Y. Cheng,

Z. Xie, L. Wang, X. Jing and F. Wang, *Adv. Funct. Mater.,* 2010, **20**, 138; [d] S.-J. Lee, J.-S. Park, M. Song, I. A. Shin, Y.-I. Kim, J. W. Lee, J.-W. Kang, Y.-S. Gal, S. Kang, J. Y. Lee, S.-H. Jung, H.-S. Kim, M.-Y. Chae and S.-H. Jin, *Adv. Funct. Mater.,* 2009, **19**, 2205; [e] R. Pode, S.-J. Lee, S.-H. Jin, S. Kim and J. H. Kwon, *J. Phys. D: Appl. Phys*., 2010, **43**, 025101; [f] M. Song, J. S. Park, M. Yoon, A. J. Kim, Y. I. Kim, Y.-S. Gal, J. W. Lee and S.-H. Jin, *J. Organomet. Chem.,* 2011, **696**, 2122; [g] J. Ding, J. Gao, Q. Fu, Y. Cheng, D. Ma and L. Wang, *Synth. Met.,* 2005, **155**, 539; [h] X. Zhang, J. Gao, C. Yang, L. Zhu, Z. Li, K. Zhang, J. Qin, H. You and D. Ma, *J. Organomet. Chem.*, 2006, **691**, 4312.

8 [a] H. J. Bae, J. Chung, H. Kim, J. Park, K. M. Lee, T.-W. Koh, Y. S. Lee, S. Yoo, Y. Do and M. H. Lee, *Inorg. Chem*., 2014, **53**, 128; [b] H. K. Dahule, S. J. Dhoble, J.-S. Ahn and R. Pode, *Journal of Physics and Chemistry of Solids,* 2011, **72**, 1524.

9 C.-Y. Sun, X.-L. Wang, X. Zhang, C. Qin, P. Li, Z.-M. Su, D.-X. Zhu, G.-G. Shan, K.-Z. Shao, H. Wu and J. Li, *Nat. Commun.,* 2013, **4**, 2717, DOI: 10.1038/ncomms3717.

10 [a] T. Kim, H. Kim, K. M. Lee, Y. S. Lee and M. H. Lee, *Inorg. Chem*., 2013, **52**, 160; [b] S.-J. Yun, H.-J. Seo, M. Song, S.-H. Jin, S. K. Kang and Y.-I. Kim, *J. Organomet. Chem*., 2013, **724**, 244.

11 J. Frey, B. F. E. Curchod, R. Scopelliti, I. Tavernelli, U. Rothlisberger, M. K. Nazeeruddin and E. Baranoff, *Dalton. Trans.,* 2014, **43**, 5667.

12 [a] J. Wang, X. Xu, Y. Tian, C. Yao and L. Li, *J. Mater. Chem. C,* 2014, **2**, 5036; [b] R. D. Chambers, Organofluorine Chemistry: Fluorinated Alkenes and Reactive Intermediates, 1997, Volume **192**.

13 D. H. Kim, N. S. Cho, H.-Y. Oh, J. H. Yang, W. S. Jeon, J. S. Park, M. C. Suh and J. H. Kwon, *Adv. Mater.,* 2011, **23**, 2721.

14 C.-H. Yang, M. Mauro, F. Polo, S. Watanabe, I. Muenster, R. Fröhlich and L. D. Cola, *Chem. Mater.,* 2012, **24**, 3684.

15 [a] X. Cao, J. Miao, M. Zhu, C. Zhong, C. Yang, H. Wu, J. Qin and Y. Cao, *Chem. Mater.,* 2015, **27**, 96; [b] S. Okada, K. Okinaka, H. Iwawaki, M. Furugori, M. Hashimoto, T. Mukaide, J. Kamatani, S. Igawa, A. Tsuboyama, T. Takiguchi and K. Ueno, *Dalton Trans.,* 2005, 1583.

16 [a] H. Sasabe and J. Kido, *Chem. Mater.,* 2011, **23**, 621; [b] Y.-J. Pu, G. Nakata, F. Satoh, H. Sasabe, D. Yokoyama and J. Kido, *Adv. Mater.,* 2012, **24**, 1765; [c] J. S. Park, J. H. Yu, W. S. Jeon, Y. H. Son, C. Kulshreshtha and J. H. Kwon, Journal of Information Display, 2011, **12**, 51.

17 J. W. Kim, S. I. You, N. H. Kim, J.-A. Yoon, K. W. Cheah, F. R. Zhu and W. Y. Kim, *Sci. Rep.,* 2014, **4**, 7009, DOI: 10.1038/srep07009.

18 H. Yersin, Highly efficient OLEDs with Phosphorescent Materials, © 2008 WILEY-VCH Verlag GmbH & Co., Page 395.

19 C.-H. Fan, P. Sun, T.-H. Su and C.-H. Cheng, *Adv. Mater.,* 2011, **23**, 2981.

20 J.-H. Lee, G. Sarada, C.-K. Moon, W. Cho, K.-H. Kim, Y. G. Park, J. Y. Lee, S.-H. Jin and J.-J. Kim, *Adv. Opt. Mater.,* 2015, **3**, 211.

21 W. Cho, G. Sarada, J.-S. Park, Y.-S. Gal, J. H. Lee and S.-H. Jin, *Org. Electron.,* 2014, **15**, 2328.

22 C. Fan, Y. Li, C. Yang, H. Wu, J. Qin and Y. Cao, *Chem. Mater.,* 2012, **24**, 4581.

23 S. Wang, B. Zhang, X. Wang, J. Ding, Z. Xie and L. Wang, *Adv. Opt. Mater.,* **2015**, DOI: 10.1002/adom.201500175.

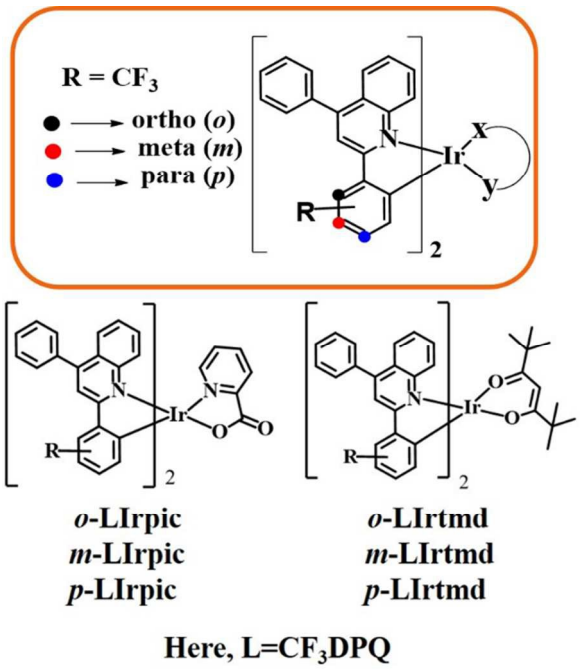

Fig. 1 Structures of the Ir(III) complexes and representation of substituent position.

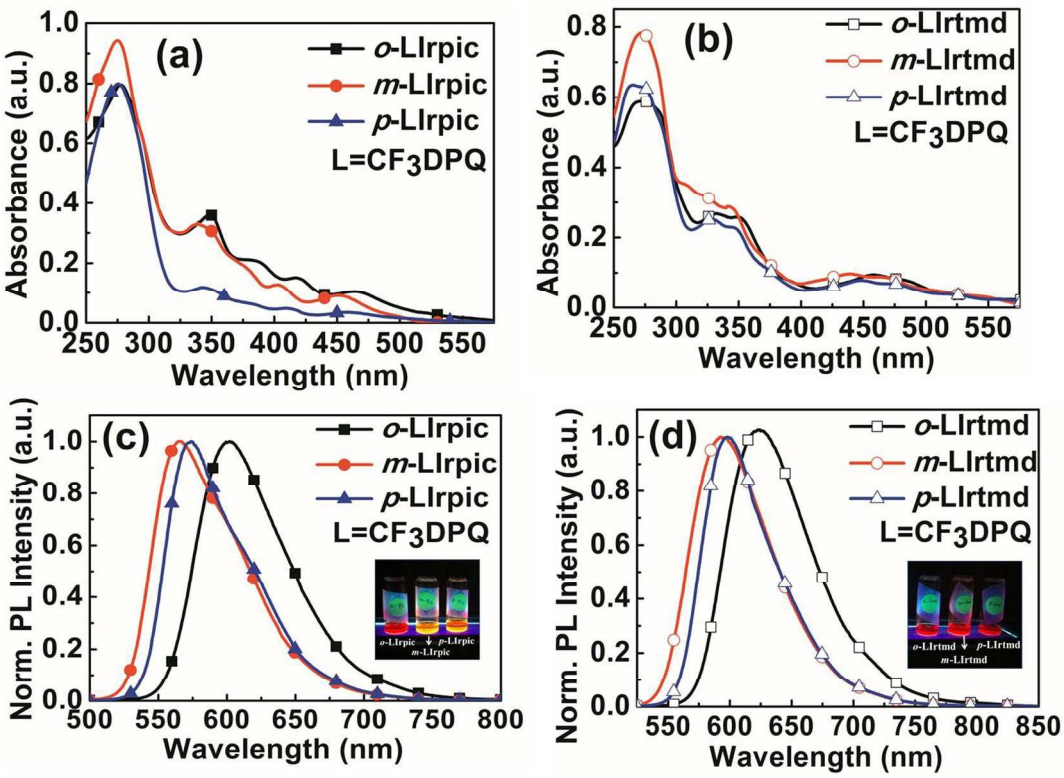

Fig. 2 (a, b) UV-visible absorption spectra; (c, d) PL spectra of the Ir(III) complexes in $CHCl_3$ solution [Insets are photographs of emission color upon UV-irradiation].

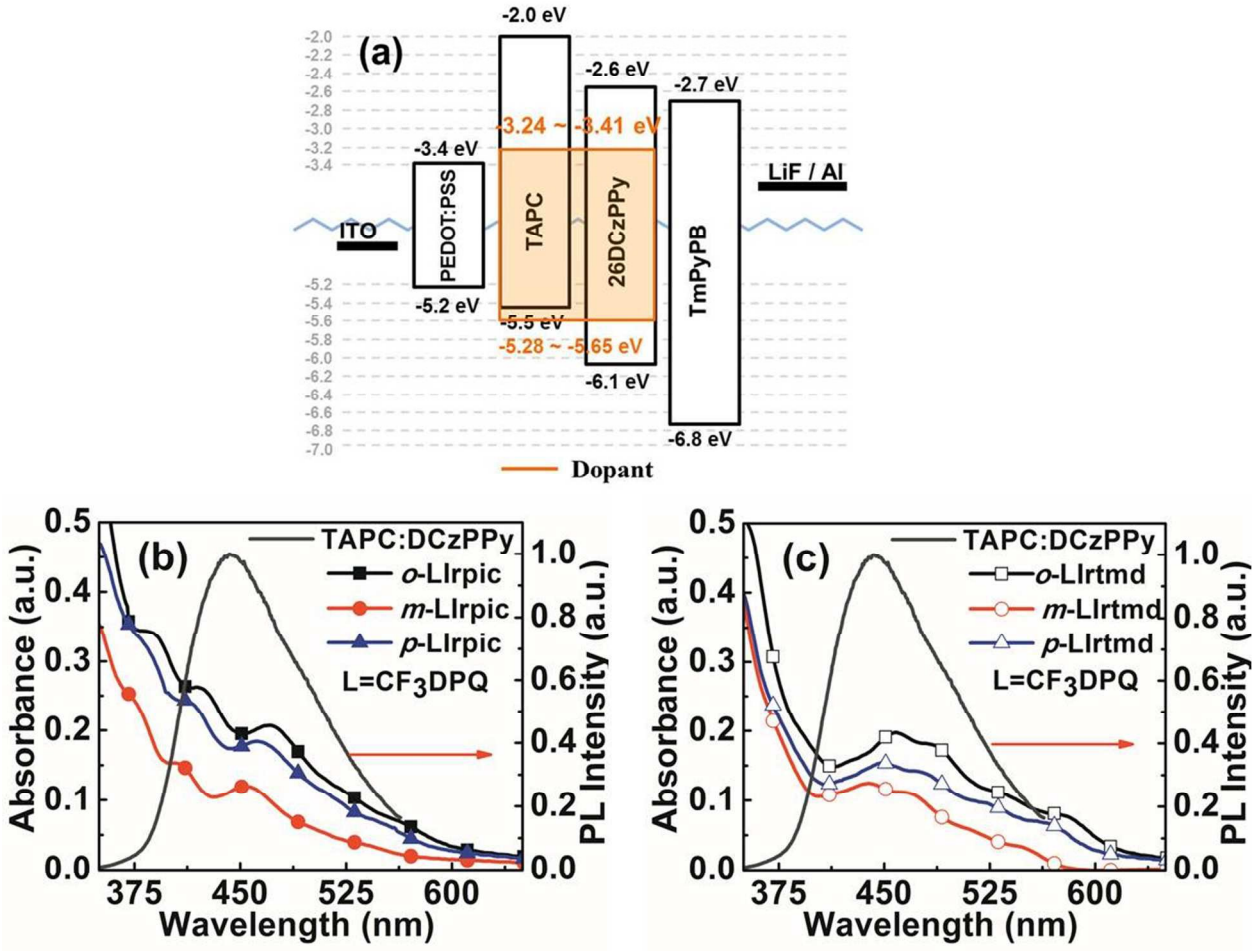

Fig. 3 (a) Device structure of monochromatic PhOLEDs; (b, c) Representation of energy transfer from the host to dopants (PL spectrum of TAPC:DCzPPy and absorption spectra of Ir(III) complexes in film state).

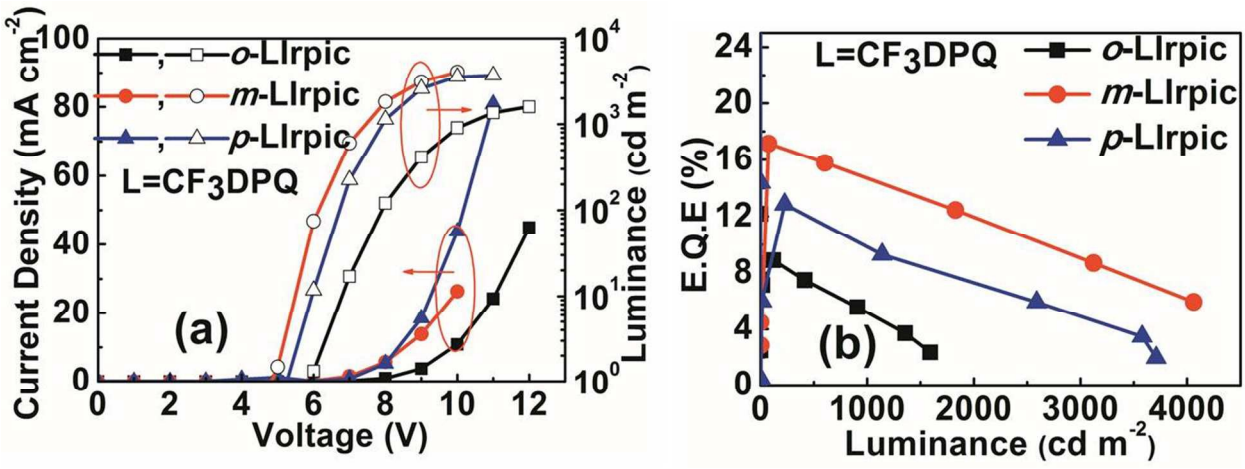

Fig. 4 (a) Current density–voltage–luminance (J–V–L); (b) EQE-luminance (η-L) characteristics of monochromatic PhOLEDs with ***o*-LIrpic**, ***m*-LIrpic**, and ***p*-LIrpic**.

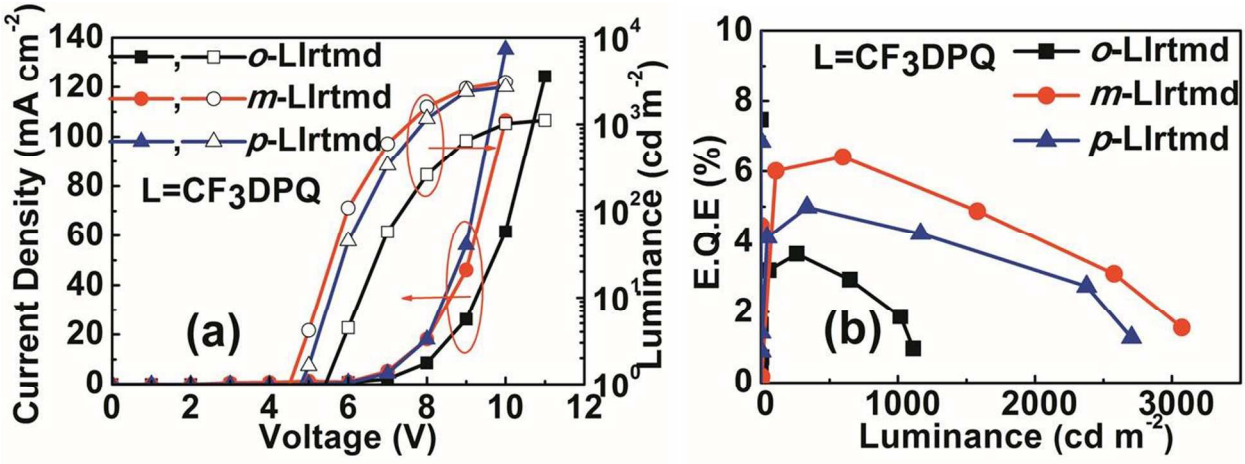

Fig. 5 (a) Current density–voltage–luminance (J–V–L); (b) EQE-luminance (η-L) characteristics of monochromatic PhOLEDs with ***o*-LIrtmd**, ***m*-LIrtmd**, and ***p*-LIrtmd**.

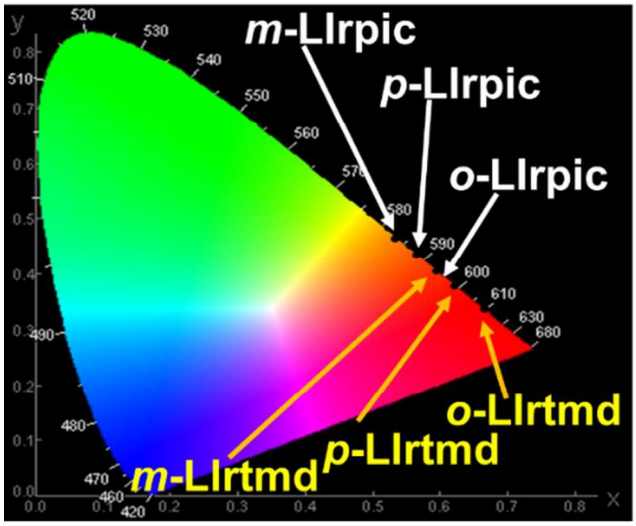

Fig. 6 1931 Commission Internationale de L'Eclairage (CIE) coordinates of the monochromatic PhOLEDs at 30 $mAcm^{-2}$.

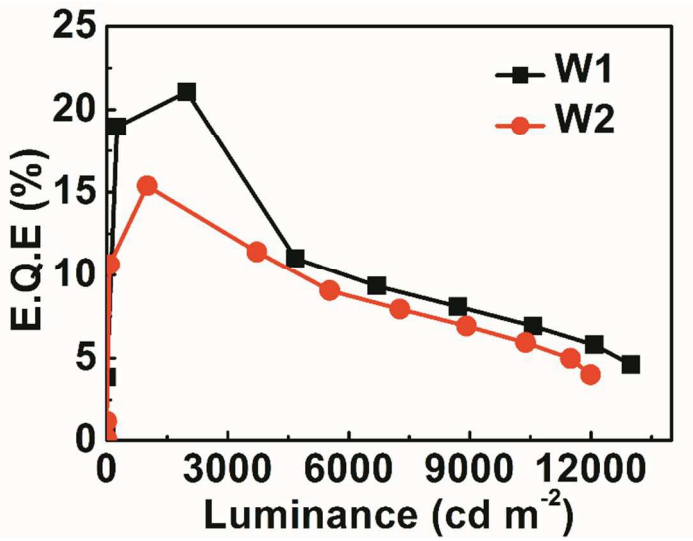

Fig. 7 EQE-luminance (η-L) characteristics of white PhOLEDs.

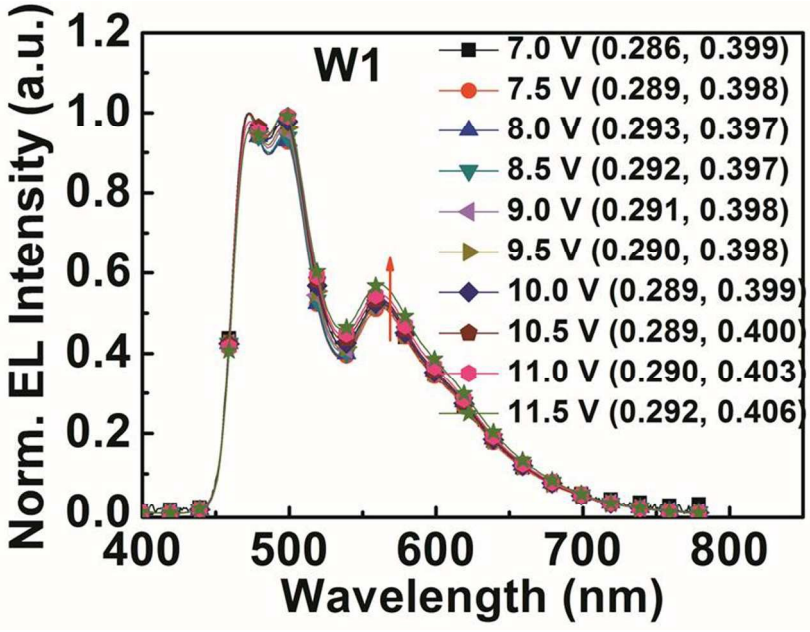

Fig. 8 EL spectra of white PhOLED at different driving voltages.

Table 1 Thermal, photophysical, and electrochemical properties of the Ir(III) complexes.

Ir(III) Complex	T_d [°C]	λ_{em} [a] [nm]	PLQY [b,c]	K_r [c] [$10^5 s^{-1}$]	K_{nr} [c] [$10^5 s^{-1}$]	τ [c,d] [μs]	E_g [e] [eV]	HOMO [f] /LUMO [g] [eV]
o-LIrpic	302	602	0.27	1.23	3.32	2.2	2.09	-5.50/-3.41
m-LIrpic	362	565	0.65	2.60	1.40	2.5	2.35	-5.65/-3.30
p-LIrpic	370	574	0.57	2.85	2.15	2.0	2.17	-5.53/- 3.36
o-LIrtmd	364	623	0.18	1.13	5.13	1.6	1.88	-5.28/- 3.40
m-LIrtmd	349	593	0.41	2.05	2.95	2.0	2.17	-5.41/- 3.24
p-LIrtmd	335	598	0.37	1.95	3.32	1.9	2.06	-5.33/- 3.27

[a] Measured in $CHCl_3$ solution at room temperature ($1x10^{-5}$M). [b] Rhodamine B ($\phi_{pl} = 0.68$) in 94% ethanol is used as reference. [c] Measured in CH_2Cl_2 at room temperature. [d] Excited state lifetimes. [e] Optical band gaps. [f] Calculated from CV. [g] Deduced from HOMO and E_g.

Table 2 EL characteristics of the monochromatic PhOLEDs with the new Ir(III) complexes

Dopant	Maximum device performance			at 1000 cdm^{-2}			EL_{max} [a]	CIE [a]
	EQE [%]	PE [lmW^{-1}]	LE [cdA^{-1}]	EQE [%]	PE [lmW^{-1}]	LE [cdA^{-1}]	[nm]	[x, y]
o-LIrpic	8.9	5.2	13.2	5.2	2.4	7.8	602	(0.613, 0.383)
m-LIrpic	17.1	23.0	43.9	14.8	16.5	38.0	572	(0.528, 0.469)
p-LIrpic	12.8	13.5	30.1	9.9	9.3	23.1	580	(0.556, 0.441)
o-LIrtmd	3.7	1.2	3.0	1.9	0.5	1.7	629	(0.663, 0.336)
m-LIrtmd	6.4	5.5	11.3	5.8	4.4	10.3	597	(0.593, 0.405)
p-LIrtmd	5.0	3.4	7.5	4.4	2.7	6.7	602	(0.622, 0.377)

[a] Values collected at a current density of 30 mAcm^{-2}.

Table 3 EL characteristics of two-component white PhOLEDs with **$(dfpmpy)_2Ir(EO_2\text{-}pic)$** [blue] and ***m*-LIrpic** [orange]

Dopant [B:O]	Maximum device performance			at 3000 cdm^{-2}			L_{max2} [cdm^{-2}]	CIE [a] [x, y]
	EQE [%]	PE [lmW^{-1}]	LE [cdA^{-1}]	EQE [%]	PE [lmW^{-1}]	LE [cdA^{-1}]		
17:0.01 (**W1**)	21.1	18.1	48.8	17.3	15.0	40.4	12992	(0.293, 0.395)
17:0.015(**W2**)	15.4	13.4	36.1	12.5	10.8	29.5	11990	(0.300, 0.406)

[a] Values collected at a current density of 30 $mAcm^{-2}$.

Table of Contents

The location of -CF_3 group on 2,4-diphenylquinoline based Ir(III) complexes is found to be very important for attaining high performance in solution-processed phosphorescent OLEDs.